

# Rheology of non-Newtonian glass-forming melts

## Part I *Flow–stress relations*

I. GUTZOW, A. DOBREVA

*Institute of Physical Chemistry, Bulgarian Academy of Sciences, Sofia 1040, Bulgaria*

J. SCHMELZER

*Sektion Physik, Universität Rostock, Universitätsplatz 3, Rostock 2500, Germany*

---

The stress-induced flow of non-Newtonian glass-forming systems is analysed in order to obtain a general algorithm for describing the kinetics of relaxation and retardation in glass-forming melts. It is shown that the existing empirical relations for plastic, pseudoplastic and dilatant flow can be derived in the framework of the Prandtl–Eyring potential barrier model, which is extended in order to include dilatant effects. The advantages and shortcomings of this molecular model are considered using experimental evidence on the flow of organic polymers, inorganic glasses and metal alloy glass-formers. It is shown that the mathematical formalism following from the potential barrier model can be conveniently used in order to derive the non-linear kinetics of relaxation of simple and polymer glass-forming melts.

---

### 1. Introduction

It is well known that efforts to obtain a quantitative description of the kinetics of relaxation in simple or polymer glass-forming melts, using Maxwell's equation in its classical linear formulation, have failed. An instructive example in this sense is given by the technically important process of glass annealing, i.e. the process of relaxation of strain birefringence in vitrified melts. A comprehensive summary of these problems has been given by Morey [1] (see also [2]).

In order to overcome the restrictions of Maxwell's linear kinetics of relaxation, two different empirical approaches have been employed until now.

(i) More than one relaxation time has been introduced, using a set of linear Maxwell equations. This method, described in detail by Mazurin [3], has been widely employed by Kovacs [4] (for earlier investigations see also [5]).

(ii) More complicated non-linear empirical relaxational dependences have been used and especially relations that correspond to differential equations with a time-dependent time of relaxation. A classical example in this respect gives Kohlrausch's fractional exponent formula [6] which has been introduced into silicate melt rheology by Rekhson and Mazurin [7] (see also [3, 8]). Similar time dependences have been used earlier by Jenckel [9–11] in order to describe relaxation in organic glass-forming melts. A fractional exponent formula has been also employed by Williams and Watts in describing dielectric relaxation (see [3, 8]).

A third possible approach for a more general, non-linear description of relaxation kinetics is attempted in the present investigation. According to this approach the flow–stress dependences of the system under con-

sideration, e.g. its non-Newtonian response to stress, is introduced into the equations describing its relaxation. In this way the particular rheological behaviour of the relaxing system is directly accounted for. This method has been indicated for the first time by Eyring and co-workers [12, 13] and in fact is employed in most of the present-day analysis of the flow and relaxational behaviour of polymer melts [8, 14, 15]. In our investigation, this approach will be specified and extended using existing or appropriately modified models for the flow–stress behaviour of melts.

In Part I of the present contribution, the mechanism of flow of real liquids is considered. Particular attention is given to the possibility of deriving existing empirical flow–stress relations in the framework of the same molecular model, the Prandtl–Eyring potential barrier approach. The mathematical and physical simplicity of this model and the fact that practically all known empirical flow–stress relations can be obtained from it, determined our choice. The advantages and shortcomings of this classical model are discussed, using available experimental evidence. Moreover, an attempt is made to extend the potential barrier model in order to describe the flow behaviour of dilatant liquids.

In Part II of the present contribution [16] non-linear analogues of Maxwell's (or Kelvin–Voigt's) equation are obtained, corresponding to different types of non-Newtonian flow behaviour observed in real glass-forming melts. It is also shown that existing empirical approaches in the kinetics of relaxation (including Kohlrausch's formula and similar dependences) can be explained and obtained as limiting cases of a general derivation.

## 2. Flow stress characterization of real glass-forming melts and the Prandtl–Eyring model

The basic rheological characteristics of a liquid are given by the dependence of shear rate of flow  $d\gamma/dt = \dot{\gamma}$  on shear stress  $S$  [17–20]. For Newtonian (or ideal) liquids

$$\dot{\gamma} = \frac{S}{\eta_0} \quad (1a)$$

holds, where  $\eta_0 = \text{constant}$  is the Newtonian viscosity of the melt. In the practice of rheological investigations, Equation 1a is usually fulfilled only in the limiting case  $S \rightarrow 0$ . Real liquids deviate from Equation 1a in the two possible ways:  $\dot{\gamma}$  increases either faster or slower than the linear dependence predicted by Equation 1a.

In order to retain the classical form of Equation 1a even for non-Newtonian liquids, we introduce here as usual (see, for example, [19, 20]) an apparent (or effective) value of the viscosity  $\eta(S) = \eta_{\text{app}}$  so that

$$\dot{\gamma} = \frac{S}{\eta_{\text{app}}} \quad (2)$$

When  $\eta_{\text{app}}$  is a decreasing function of  $S$ , the liquid is called pseudoplastic (or in polymer literature, shear thinning) and when  $\eta_{\text{app}}$  increases with increasing  $S$  the liquid is termed dilatant (or in polymer technology, shear thickening). The pseudoplasticity and dilatancy of liquids are illustrated in Fig. 1a and b. The  $\dot{\gamma}(S)$  function of Bingham's plastic body [17] is also given in the same figure as a limiting case of pseudoplasticity. Bingham's  $\dot{\gamma}$  function has the form

$$\dot{\gamma} = \frac{1}{\eta_0} (S - S_0) \quad (1b)$$

It is seen that according to it there is a distinct stress limit,  $S_0$ , below which no flow is possible (Fig. 1c).

A molecular model, first developed by Prandtl [21] (see also [22]) and then derived in terms of the Absolute Rate Theory by Eyring [19, 20, 23, 24] gives a simple and instructive explanation for the non-Newtonian behaviour of pseudoplastic materials. Prandtl and Eyring assumed that in a liquid subjected to tangential stress the activation energy barrier,  $U(T)$ , for self-diffusion decreases in the direction of

the applied stress by the quantity  $\Delta\varepsilon$  proportional to  $S$ . In the opposite direction,  $U(T)$  increases by the same quantity,  $\Delta\varepsilon$  (Fig. 2). In this way the rate of net flow,  $\dot{\gamma}$ , in the direction of the applied stress becomes

$$\dot{\gamma} = \frac{2D}{d^2} \sinh\left(\frac{d^3}{2kT} S\right) \quad (3)$$

where

$$D = d^2 \tau^* \exp\left(-\frac{U(T)}{kT}\right) \quad (4)$$

is the self-diffusion coefficient of the building units of the liquid,  $k$  is Boltzmann's constant and  $U(T)$  is the respective activation energy at temperature  $T$  for the melt at rest. With  $\tau^*$  is denoted the reciprocal of the frequency of eigen vibrations of the building units of the melt. The structural units responsible for the flow occupy the volume  $d^3 = V$  (the so-called "viscous volume"). This viscous volume should be proportional to the volume  $d_0^3 = V_0$  of the building units of the system. Using the Stokes–Einstein equation in the form derived in the framework of the Absolute Rate Theory

$$D = \frac{kT}{d\eta_0} \quad (5)$$

Equation 3 can be written as

$$\dot{\gamma} = \frac{A}{\eta_0} \sinh(aS) \quad (6a)$$

According to the above considerations, given in more detail by Glasstone *et al.* [23],  $a = d^3/2kT$  and  $A = 1/a$ .

In Eyring's original derivation it was assumed that  $U(T) = U_0 = \text{constant}$ . However, on introducing  $\eta_0$  through Equation 5, more complicated  $U(T)$  dependences (e.g. corresponding to the Vogel–Fulcher–Tammann formula) have to be anticipated.

In the framework of a more general formulation of the Prandtl–Eyring approach [25], Equation 6a can be written in the form

$$\dot{\gamma} = \frac{A}{\eta_0 f^*} \sinh[f^* a(S - S_0)] \quad (6b)$$

to include also systems with a plastic stress limit,  $S_0$ . The factor  $f^*$  gives the reciprocal of the fractional area

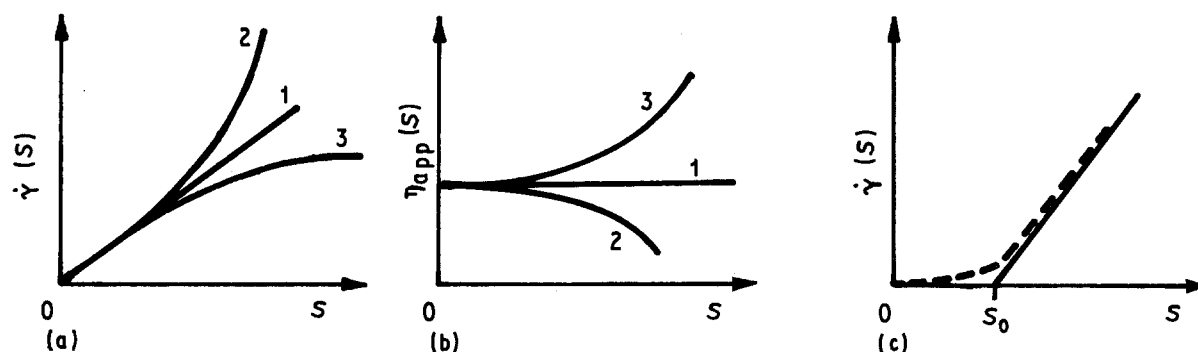


Figure 1 Flow behaviour of liquids (shown schematically). (a) Shear rate–shear stress dependences. 1, Newtonian fluid; 2, pseudoplastic liquid; 3, dilatant melt. (b) Dependence of the apparent viscosity on stress: 1, Newtonian; 2, pseudoplastic; 3, dilatant. (c) Shear rate–shear stress dependences for pseudoplastic liquids (---) and Bingham's body approximation (—).

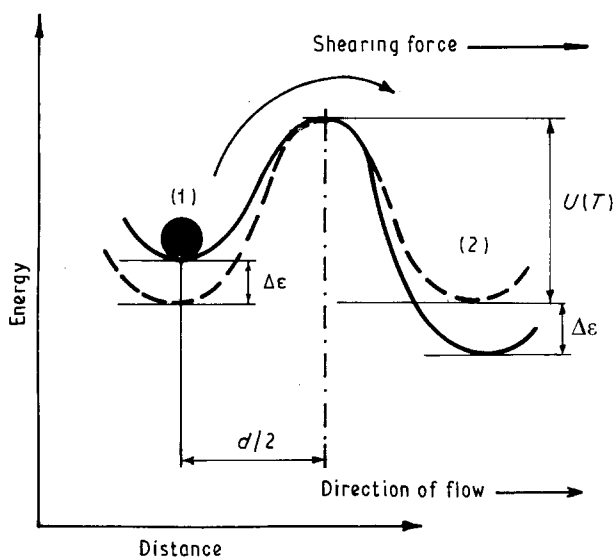


Figure 2 The Prandtl-Eyring model for the change of activation energy profile in a pseudoplastic liquid under applied stress. Liquid at rest (---); the two positions of the spherical structural unit are separated by an activation barrier  $U(T)$ . The activation energy profile is defined  $\Delta\epsilon = f^*(d^3/2kT)S$  (—).

occupied by non-Newtonian flow units to the surface of inert (or Newtonian) structural elements [25]. Thus,  $f^*$  accounts for the number of structural units which take part in the flow process.

The Prandtl-Eyring potential barrier model has been a subject of a serious criticism [26, 27]. Most objections are connected with its application in the flow of polymer solutions and melts where the complicated hydrodynamics of movement of more or less entangled polymer coils, as described by Bueche's free-draining coil model [19, 28, 29] or by more recent tube-flow models [14, 15, 30] seem to dominate the process and even to exclude the necessity of a potential barrier approach.

The weakest point of the Prandtl-Eyring formalism is the nature of the viscous volume,  $V$ , and its connection with the volume of real structural units,  $V_0$ , in the system. It appears (see Section 5 and [25]) that in treating flow in polymer melts, hundreds and even thousands of structural units are responsible for the flow process.

In spite of this criticism the following arguments were decisive in adopting the Prandtl-Eyring potential barrier model as a starting point in the present investigation:

(i) The general applicability of the activated complex idea: it can be applied in principle to any system (melt, crystal, solution). This cannot be said for the more specific flow models mentioned above, derived for particular systems (e.g. tube and coil models for polymers).

(ii) The relatively simple mathematical formulations describing the  $\dot{\gamma}(S)$  dependences: it is shown in Part II [16] that the introduction of flow-stress relations, derived from Equation 6, into the relaxational equations allows direct integration without further approximations.

(iii) The possibility to interrelate the existing flow-stress equations: it is easy to establish connections between this model and the variety of existing flow-stress formulae (even with those predicted by the polymer molecular theories).

(iv) The possibility to extend the Prandtl-Eyring approach in order to describe the flow of dilatant materials: the Prandtl-Eyring potential barrier model even in its most elaborate form (see Equation 6b and [25]) is applicable only to pseudoplastic liquids. The polymer models mentioned [19, 28, 30] also refer only to pseudoplastic flow. However, a relatively simple extension can be made of the Prandtl-Eyring model in order to include the flow of dilatant liquids. This extension is attempted in the next section.

Let us consider first the connection between the Prandtl-Eyring model and existing empirical relations.

Accounting for the well-known approximations of the hyperbolic sine function (see, for example, [31]) i.e.

$$\sinh(x) \approx x \quad \text{for } 0 < x \ll 1 \quad (7a)$$

$$\sinh(x) \approx x \left(1 + \frac{1}{6}x^2\right) \quad \text{for } x < 1 \quad (7b)$$

$$\sinh(x) \approx \frac{1}{2} \exp(x) \quad \text{for } x \gg 1 \quad (7c)$$

it can be easily seen that Equation 6a leads at  $aS \rightarrow 0$  to Newton's law and Equation 6b to the Equation 1b for Bingham's plastic body. Further, Gee and Lion's formula (see, for example, [32])

$$\dot{\gamma} = A_1(1 + b_0 S^{m-1}) \frac{S}{\eta_0} \quad (8)$$

can be obtained from Equations 6 and 7b with  $A_1 = 1$ ,  $m = 3$ ,  $b_0 = a^2/6$ . Another illustration is the equation of de Waele-Ostwald [17, 33, 34]

$$\dot{\gamma} = A_2(S^{n-1}) \frac{S}{\eta_0} \quad (9)$$

where  $A_2$  is a constant. Usually, Equation 9 (sometimes referred to as Reiner's formula [35]) is used to describe the flow of polymer melts in practical terms.

Equation 9 follows from Equation 6a taking into account that for  $0.5 < x < 1.5$  the optimal approximation to the  $\sinh(x)$  function is the semi-cubic parabola which specifies  $n$  as  $n \approx 1.5$  ( $Y = Cx^{3/2}$  with  $C \approx 1.2$ ) (Fig. 3). For the same interval, Equation 7b gives a close approximation to the  $\sinh x$  function; the connection between Equations 8 and 9 is also obvious. At higher  $x$  values (for  $1.5 < x < 3$ ) a more appropriate approximation to the  $\sinh$  function is a higher  $n$ -valued parabola (e.g.  $Y = 0.6x^{5/2}$ ). In this sense it appears that the value of  $n$  in Ostwald's (or Reiner's) formula has, in fact, no definite physical meaning and changes from 1 to higher  $n$  values in dependence of the particular interval of  $aS$  values employed.

At very high  $aS$  values (i.e. at  $aS \gg 1$ ) by virtue of Equation 7c we have from Equation 6a

$$\ln \dot{\gamma} \approx \ln \frac{A}{\eta_0} + \frac{1}{2} a^2 S \quad (10)$$

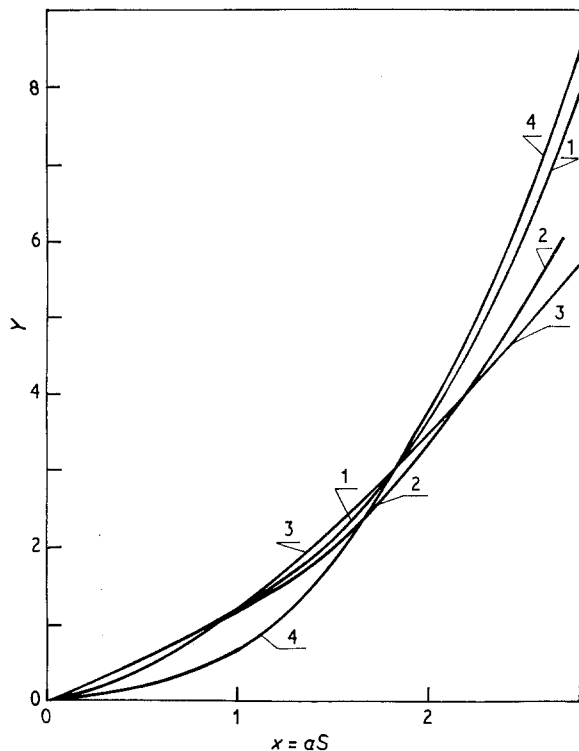


Figure 3 The sinh function and its approximations. 1, sinh function; 2, Taylor's second term expansion of  $\sinh x$  (Equation 7b); 3, Semi-cubic parabola  $Y = 1.2x^{3/2}$ ; 4, 5/2 parabola  $Y = 0.6x^{5/2}$ .

as is frequently observed in the flow of polymer melts. This formula gives a  $\dot{\gamma}(S)$  dependence proposed by Bartenev [36] (see also [20]) who used the concept that non-Newtonian flow behaviour results from a process of structural change under stress.

The Prandtl–Eyring molecular model and Equations 6a and b cannot give an explanation for the dilatant behaviour of liquids. In terms of the de Waele–Ostwald empirical equation (Equation 9, which in this sense is, in fact, more general than Equations 6a and b) dilatant behaviour of liquids follows at  $n < 1$ . Thus for  $n = 1/2$  another empirical relation

$$\begin{aligned} \dot{\gamma} &= \frac{A_2}{\eta_0} S^{1/2} \\ &= \left( \frac{A_2}{S^{1/2}} \right) \frac{S}{\eta_0} \end{aligned} \quad (11)$$

known as Darcy's formula is obtained (see [33]).

Moreover by using Equations 6a and b or the dependences derived from them, the possibility of transitions from pseudoplastic to dilatant behaviour (or the reverse transition) is excluded. Such transitions, however, are observed in the flow behaviour of real liquids when greater  $S$  intervals are investigated. Examples in this respect can be found in the literature [33, 34] (see also [25]) the most striking of them being water and aqueous colloid solutions.

### 3. Generalized molecular model: combined dilatant and pseudoplastic behaviour

Molecular dynamic simulation indicates that by applying shear stress to a simple liquid constituted of

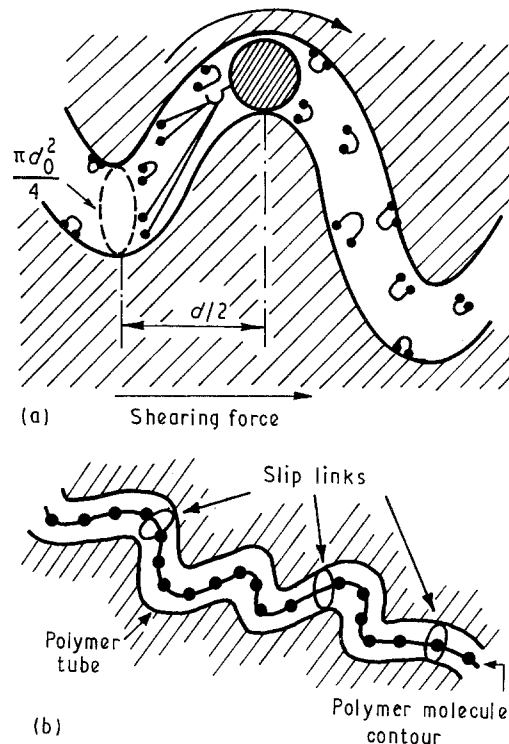


Figure 4 Dilatant behaviour and tube models of flow of simple and polymer melts. (a) Jump of a molecule flowing in an entanglement-saturated tube over a potential barrier at applied shearing force. Two molecular entanglements have been activated and they hamper the jump of the molecule under consideration. (b) Polymer molecule contour flowing in a hypothetical tube with slip links.

billiard-like spherical molecules, an ordering and layering process takes place which enhances flow [37]. Similar effects follow in the framework of the coil and tube models of polymer solutions [14, 15, 28, 29]. In terms of the Prandtl–Eyring model this enhancement is described by a decrease of the potential barrier in the direction of stress (Equations 6a and b) and thus the flow is facilitated. Consequently, pseudoplastic behaviour results and known  $\dot{\gamma}(S)$  functions given with Equations 6, 8, 9, 10 are obtained.

In order to account for the dilatancy in the flow of real liquids we have to consider additional molecular effects which introduced into the Prandtl–Eyring model could lead to a decrease of the flow rate, e.g. by an increase of the overall activation energy with increasing flow rate  $\dot{\gamma}$ .

Such effects may be described generally as the creation of additional molecular disorder and increased intermolecular interaction (or friction) when a complicated flow unit of the liquid “jumps” over Eyring's potential barrier under stress.

Let us consider a model according to which every molecule of the system flows through an imaginary tube representing the collective effect of all surrounding molecules and that some sort of entanglements strayed in the tube are activated upon flow and that for a given molecular structure the number of molecular bonds (or entanglements) increases with increasing flow rate  $\dot{\gamma}$ .

Thus the applied shearing force,  $S$ , in general lowers the potential barrier but disorder and additional molecular friction can be also caused by the increased

flow velocity and may thus hamper the jump over the potential barrier, especially for asymmetric complex molecules, which may be "hooked" by the tube entanglements as illustrated in a simplified scheme in Fig. 4.

More generally, asymmetric molecules may be oriented by increasing flow velocity, thus diminishing viscosity (pseudoplastic effect); however, entanglement formation may be facilitated between oriented molecules and viscosity may increase (dilatant effect). A possible mechanical model schematically illustrating such a situation in a liquid composed of asymmetric molecules is given in Fig. 5.

In the case of complicated polymer structures it can be also assumed that chains wriggling in the hypothetical tube may be trapped by an increasing number of imaginary slip links through which the contour of the chain passes with increased difficulty at increasing flow rate (Fig. 4b).

To this and similar models the same scheme of considerations can be applied. Let us assume, for example, that the initial concentration of active entanglements (or slip links) per unit length in the liquid tube surrounding the contour of simple or chain-like molecules is  $\xi N_0$  at  $\dot{\gamma} = 0$ . The steric factor  $0 < \xi < 1$  reflects the flexibility and the complexity of the structural units (or polymer segments) of the melt and  $N_0$  is the concentration of these units at rest. Thus for the structural unit with a contact surface area  $\pi d_0^2$ , occupying the cylindrical volume  $\pi d_0^3/4$ , the number of expected entanglement contacts (or slip links) at rest is approximately equal to  $\xi N_0 \pi d_0^3$ .

Suppose that for the considered structures the number of entanglements increases proportionally to the volume  $\pi d_0^2 t_0 d_0 \dot{\gamma}/4$  swept out by the jumping molecule during the time,  $t_0$ , necessary for the jump itself.

Let  $E_0$  be the increased energy with which the entanglement (or slip link) binds the jumping molecule (or polymer segment) and thus inhibits the molecular movement. The jump of every structural unit through the potential barrier takes on average the time of eigen vibrations,  $\tau^*$ , of the molecules [23] (i.e.  $t_0 = \tau^*$ ). Thus the number of flow-created entanglements per unit volume of the melt is

$$N = \frac{1}{4} \pi d_0^3 N_0 \xi \tau^* \dot{\gamma} \quad (12)$$

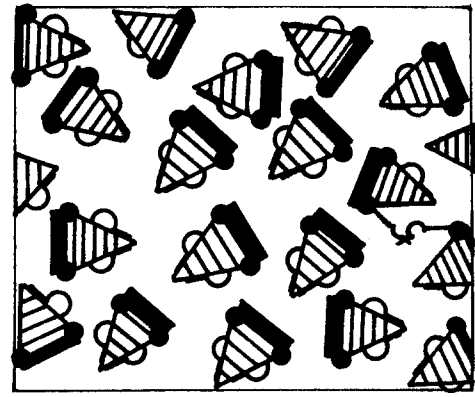
and thus the activation energy for the discussed entanglement limited viscous flow becomes

$$Q(T) = E_0 N_0 \xi \pi d_0^3 \left( 1 + \frac{1}{4} \tau^* \dot{\gamma} \right) \quad (13)$$

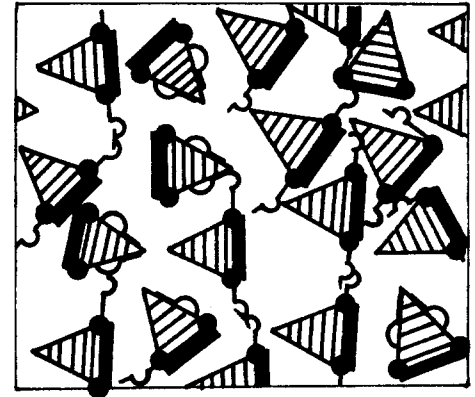
Introducing  $Q_0(T) = E_0 N_0 \xi \pi d_0^3$  into  $U(T)$  in Equation 4 and denoting  $\Gamma_0 = E_0 N_0 \xi \pi d_0^3 \tau^*/4kT$ , we must write, instead of Equations 3 and 6, a new extended  $\dot{\gamma}(S)$  dependence. Accounting for Equation 5, it can be represented in the form

$$\dot{\gamma} = \frac{A}{\eta_0} \sinh(aS) \exp(-\Gamma_0 \dot{\gamma}) \quad (14)$$

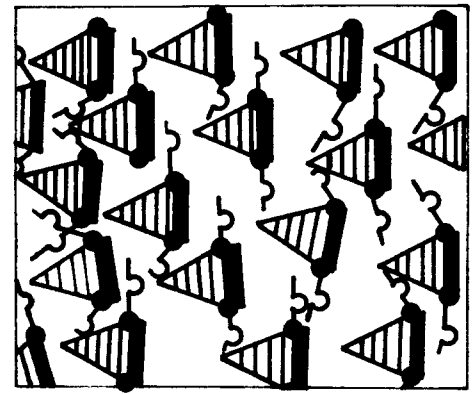
In this equation the sinh function accounts for pseudoplasticity and the exponent for dilatant effects.



(a)



(b)



(c)

Direction of flow

Figure 5 Molecular model illustrating steric entanglement effects in dilatant flow behaviour. (a) Liquid at rest: no orientation of the asymmetric molecules, only one chance entanglement is seen. (b) Liquid at moderate flow velocity: beginning of orientation, moderate activation of entanglements. (c) Fast flow: pronounced orientational effects, full activation of entanglements.

The  $\dot{\gamma}(S)$  dependence resulting from Equation 14 is illustrated in Fig. 6a for different  $\Gamma_0$  values. It is seen that the higher the value of  $\Gamma_0$  ( $B_0$  in Fig. 6a is proportional to  $\Gamma_0$ ), the more pronounced is the dilatant behaviour expected. At higher  $aS$  values, pseudoplastic flow again follows, depending on the value of  $\Gamma_0$ .

In considering Equation 14, two limiting cases can be distinguished.

(i) For small  $\Gamma_0 \dot{\gamma}$  values (i.e. for  $\Gamma_0 \dot{\gamma} \ll 1$ ), the exponent in Equation 14 can be approximated by

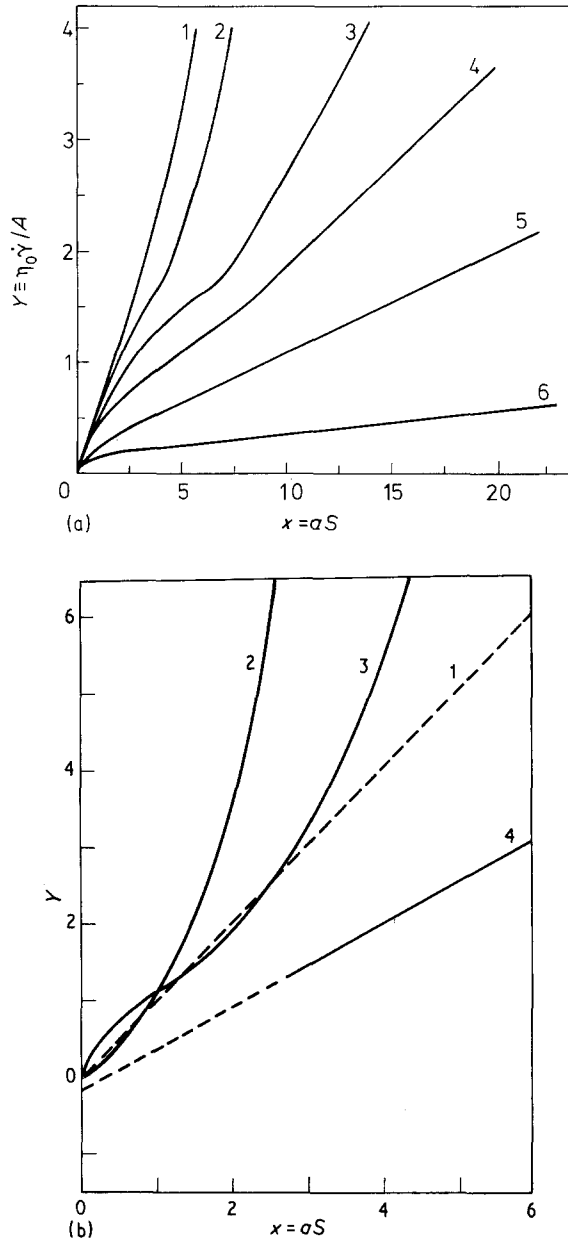


Figure 6 Different types of flow behaviour according to the generalized molecular model (Equation 14) in coordinates  $Y = \dot{\gamma}\eta_0/A$  versus  $x = aS$ . (a)  $\dot{\gamma}(S)$  dependences following from Equation 14 for different values of the parameter  $B_0 = A/\eta_0\Gamma_0$ : 1,  $B_0 = 0$ ; 2,  $B_0 = 0.1$ ; 3,  $B_0 = 0.5$ ; 4,  $B_0 = 1$ ; 5,  $B_0 = 3$ ; 6,  $B_0 = 10$ . (b) 1, Newtonian behaviour (---); 2, sinh function according to Equation 6a; 3, the approximation given with Equation 15 at  $(\eta_0\Gamma_0^*/A)^{1/2} = 1$ ; 4,  $\dot{\gamma}(S)$  dependence according to Equation 17c for large  $aS$  values at  $(1/\Gamma_0 = 1)$ .

$\exp(-\Gamma_0\dot{\gamma}) \approx (1 - \Gamma_0\dot{\gamma}) \approx (1 + \Gamma_0\dot{\gamma})^{-1} \approx 1/\Gamma_0^*\dot{\gamma}$  where  $\Gamma_0^*$  is an appropriately chosen constant. In this way Equation 14 can be written as

$$\dot{\gamma} \approx \left( \frac{A}{\eta_0\Gamma_0^*} \sinh(aS) \right)^{1/2} \quad (15)$$

This approximation is illustrated in Fig. 6b.

It is evident (see Fig. 6) that Equation 15 provides through a combination of a sinh function and a square root, a simple description of a possible transition from dilatant to pseudoplastic behaviour. At  $aS \ll 1$ , Equation 15 gives directly Darcy's equation, Equation 11.

When  $\Gamma_0 \approx 0$  (i.e. when entanglement effects can be neglected either because of  $N_0 \approx 0$  or of  $\xi \approx 0$ ) the

general dependence (Equation 14) gives as a particular case the Prandtl-Eyring equation (Equation 6a) and the already discussed  $\dot{\gamma}(S)$  relations describing pseudoplastic behaviour (i.e. the de Waele-Ostwald formula with  $n > 1$ , the relation of Gee and Lion and Bartenev's equation).

When  $aS \ll 1$  with  $\exp(-\Gamma_0\dot{\gamma}) \approx (1 + \Gamma_0\dot{\gamma})^{-1}$ , Equation 14 leads to a  $\dot{\gamma}(S)$  dependence proposed many years ago by Reynolds for describing the dilatant behaviour of suspensions [32]. According to Reynolds' "wet sand model", the apparent viscosity,  $\eta_{app}$ , increases at increasing flow rate as

$$\eta_{app} = \eta_0(1 + \phi) \quad (16)$$

i.e. as in an Einstein suspension with diminishing free volume. Here  $\phi$  is given by the product  $\phi = \Gamma_0\dot{\gamma}$ .

(ii) For high  $\Gamma_0\dot{\gamma}$  values (i.e. at  $\Gamma_0\dot{\gamma} > 1$ , when  $\dot{\gamma}$  can be neglected as compared with  $\exp(\Gamma_0\dot{\gamma})$ , Equation 14 leads to another possible approximation

$$\dot{\gamma} \approx \frac{1}{\Gamma_0} \left[ \ln \frac{A}{\eta_0} + \ln(\sinh aS) \right] \quad (17a)$$

Accounting for Equation 7a, the above relation gives for small  $aS$  values

$$\dot{\gamma} \approx \frac{1}{\Gamma_0} \left( \ln \frac{A}{\eta_0} + \ln aS \right) \quad (17b)$$

and with Equation 7c, for high  $aS$  values

$$\dot{\gamma} \approx \frac{1}{\Gamma_0} \left( \ln \frac{A}{\eta_0} + \frac{1}{2} aS \right) \quad (17c)$$

This approximation is also illustrated in Fig. 6b. It is seen that at  $\Gamma_0\dot{\gamma} > 1$ , Equation 14 (or Equations 17a-c) determines a pseudoplastic behaviour (Equation 17a) followed by a quasi-Newtonian dependence at high  $aS$  values. One of the modifications of Eyring's theory, the Powell-Eyring equation [20], also describes a similar quasi-Newtonian  $\dot{\gamma}(S)$  dependence.

The present analysis shows that our generalized formula, Equation 14, describes pseudoplasticity (or pseudoplasticity with an initial plastic limit if Equation 6b is used), dilatancy as well as the possible transformations between these two modes of flow.

#### 4. Temperature dependence of the parameter $a$

The analysis of the temperature dependence of the parameter  $a$  appearing in Equations 6 and 14 could give additional insight into the physical basis of the Prandtl-Eyring model.

In this original derivation Eyring has assumed that the viscous volume is a constant [23], i.e.  $d^3 = d_0^3$  where  $d_0^3$  is determined by the molar volume of the structural unit  $V_m$  as  $d_0^3 = V_m/N_a$ ,  $N_a$  being Avogadro's number. In a further approximation it was assumed (as for gases) that  $V_m(T) \sim RT$  [25] and thus the parameter  $a$  becomes a constant. From a general point of view it should be expected, however, that the viscous volume  $d^3$  should be determined by a more realistic temperature dependence of the molar volume  $V_m(T)$  of the liquid. Using the well-known Mendeleeff

formula (in the form given by Oswald and Davies, cf. [38])

$$V_m(T) = \frac{V_m^0}{T^* - T} \quad (18)$$

we should expect that, in fact, the following equation should hold

$$a(T) \approx \frac{V_m^0}{2RT} \left( \frac{1}{T^* - T} \right) \quad (19)$$

where  $V_m^0$  is the molar volume of the flow unit at  $T = 0$  K.

According to Partington [38],  $T^*$  in Equation 19 can be evaluated from the critical temperature,  $T_c$ , of the liquid under consideration as

$$T^* \approx 2T_c \quad (20)$$

In this way with  $T_c \approx (\frac{5}{3} - \frac{4}{3}) T_m$  (as  $T_c$  is usually estimated) and the Beaman-Kauzmann rule connecting melting temperature,  $T_m$ , with the vitrification temperature of the melt,  $T_g$ , as  $T_g \approx \frac{2}{3} T_m$ , it follows that  $T^* \approx (5 - 4) T_g$ . In this way  $T^*$  can be connected with molecular constants known for every glass-forming melt.

## 5. Experimental evidence of the mechanism of viscous flow in simple and polymer glass-forming melts

The general method for examining the flow behaviour of a viscous system is the analysis of  $\dot{\gamma}(S)$  curves. The first systematic investigations in this respect were done by Ostwald with colloid solutions [17, 33, 34]. In most cases, typical pseudoplastic behaviour was observed and described in terms of the de Waele-Ostwald equation (Equation 9). It was found that for aqueous colloid solutions the exponent  $n$  ranges from 1.3–1.8. (cf. the experimental evidence collected by Ostwald [33, 34] for 25 different sols). For  $aS < 1$ , the mean value of  $n$  is centred according to our prediction around the semi-cubic parabola  $n$  value ( $n = 1.5$ ). With increasing sol concentration, the value of the Newtonian viscosity,  $\eta_0$ , increases according to the already discussed Einstein formula [33] but the value of  $n$  remains unchanged. Ostwald also reports several examples for transition from dilatant to pseudoplastic behaviour with  $\dot{\gamma}(S)$  dependences having a similar course as that predicted by Equations 15 and 17.

The first attempt to correlate the experiment with the derivations of the potential barrier theory was done by Eyring and his co-workers [23, 25]. They found that a number of pseudoplastic materials (rubber, several organic polymer melts and solutions, metal alloys, etc.) obey Equations 6a and b. A further step in this respect was undertaken by Li and Uhlmann [26] who investigated the stress-induced pseudoplastic flow of a  $Rb_2O/SiO_2$  melt and critically analysed the results in terms of the Prandtl-Eyring model. Again qualitative agreement with Equation 6a was found.

Most of the experimental evidence on the flow of organic polymer solutions collected in recent years

has been examined only in the framework of the mentioned specific polymer molecular theories. Accounts in this respect may be found in the literature [19, 20, 29]. A qualitative (or even semi-quantitative) coincidence with the predictions of the free-draining coil or tube model theories [14, 15, 28, 30] was established.

Fig. 7 illustrates the flow behaviour of a typical organic polymer—poly(decamethylene terephthalate) (PDMT). The  $\dot{\gamma}(S)$  curves for this polymer were obtained in our laboratory by using a Searle-type rotational viscometer [39]. It is seen from the figure that at small shear stresses, true Newtonian flow is observed, while at  $S \approx 12000$  Pa a deviation from the linear proportionality begins. This prolonged linear  $\dot{\gamma}(S)$  dependence may be regarded as an indication for the validity of Equation 6a (cf., and the course of the sinh function in Fig. 3).

Figs 8 and 9 show flow–stress curves of a typical inorganic glass-forming melt,  $0.3Li_2O \cdot 0.2Na_2O \cdot 0.5Pb_2O_5$  as reported by Wäsche and Brückner [40] and for a metallic glass-forming melt with the composition  $0.82Fe-0.18B$  [41], respectively. The analysis in terms of the de Waele-Ostwald equation (Equation 9) gives again  $n = 1.5$  for the two systems and the Prandtl-Eyring formula (Equations 6a and b) can be conveniently used to describe the flow.

The flow–stress curves for another typical organic polymer glass-forming melt, poly(methyl methacrylate), are presented in Fig. 10 according to the experimental evidence given by Gul and Kuleznev [42]. It is seen that when  $S$  changes over several decades, the de Waele-Ostwald formula becomes a poor approximation. However, as expected, the Prandtl-Eyring equation describes with sufficient accuracy the  $\dot{\gamma}(S)$  behaviour of this polymer melt in the investigated wide range of stress deformations.

The values of the parameter  $a$  in Eyring's Equations 6a and b can be estimated from the point of departure of the  $\dot{\gamma}(S)$  curves from linearity, where according to Equation 7,  $aS \approx 1-0.75$  (see also [20, 26]). In order to determine more exactly the values of  $a$  and  $\eta_0$  in terms of Equation 6a, we employed a conventional computer program for non-linear regression analysis. It was found that the  $\eta_0$  values calculated in this way correspond to the Newtonian viscosity determined by the standard graphical extrapolation in coordinates  $\log \eta_{app}$  versus  $\log S$  (see Fig. 10b).

The  $\dot{\gamma}(S)$  dependences for another organic polymer system, the alternating tetrafluoroethylene ethylene copolymer (trade name Tefzel), filled with 0.3%  $TiO_2$  are given in Fig. 11 for a broader temperature interval also according to our measurements [39]. In coordinates  $\log \dot{\gamma}$  versus  $\log S$  by virtue of the de Waele-Ostwald formula for the Tefzel melts, parallel straight lines are obtained with a slope again equal to 1.5. However, a more adequate description of the same experimental results is obtained with the Prandtl-Eyring equation (Fig. 11b). Moreover, the computer analysis in terms of Equation 6a gives a temperature dependence for the parameter  $a$  in accordance with Equation 19 and Mendeleeff's formula for  $V_m(T)$  (Fig. 11c).

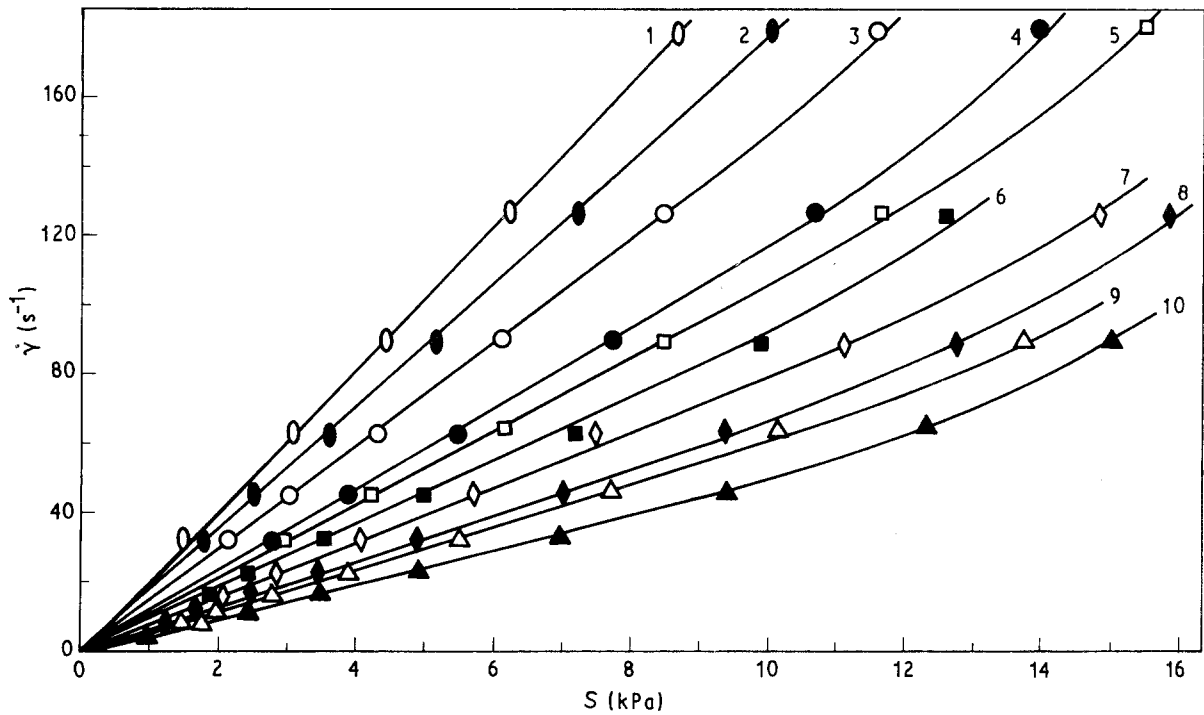


Figure 7 Flow-stress behaviour of polydecamethylene terephthalate according to Dobreva *et al.* [39]: 1, 449 K; 2, 439 K; 3, 433 K; 4, 425 K; 5, 420 K; 6, 415 K; 7, 409 K; 8, 403 K; 9, 401 K; 10, 397 K; 11, 393 K.

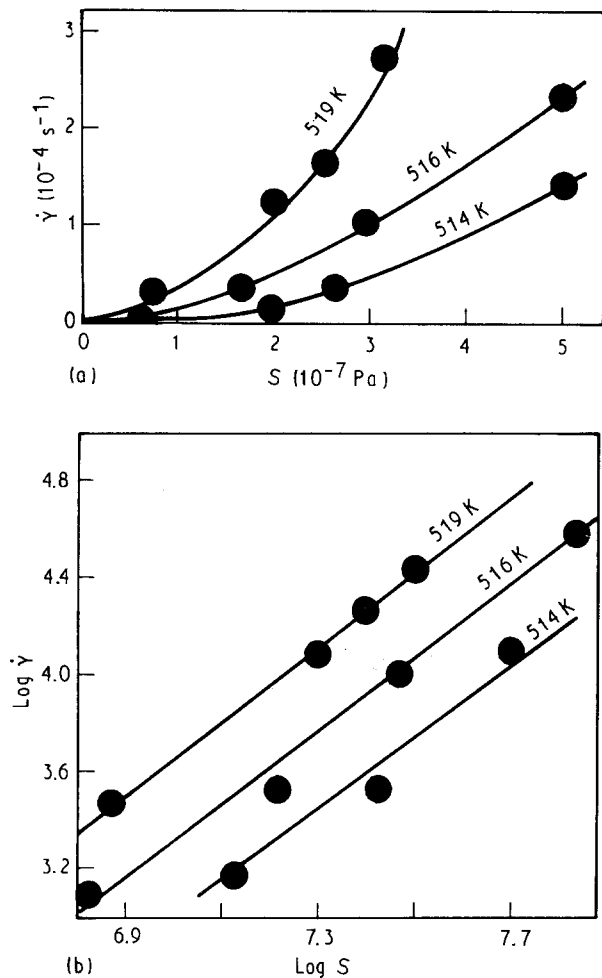


Figure 8 Viscous flow of  $0.3\text{Li}_2\text{O}\cdot 0.2\text{Na}_2\text{O}\cdot 0.5\text{P}_2\text{O}_5$  melts. (a)  $\dot{\gamma}(S)$  curves after Wäsche and Brückner [40] at three different temperatures indicated on each curve. (b) The same data in  $\log \dot{\gamma}$  versus  $\log S$  according to the de Waele-Ostwald Equation with  $n = 1.5$ .

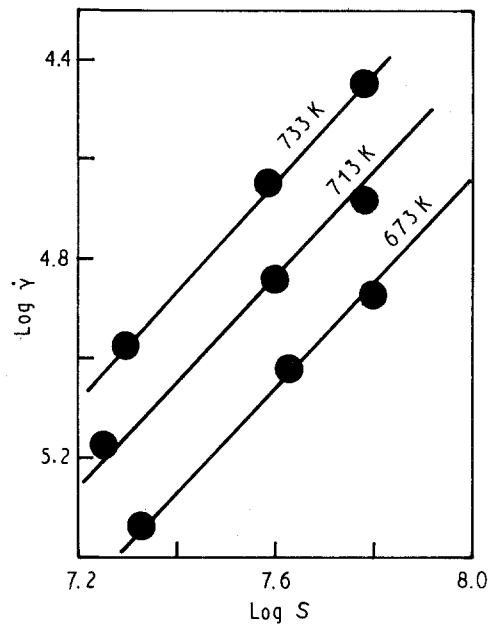


Figure 9 De Waele-Ostwald plot of experimental data for a metallic alloy glass-forming melt with composition  $0.82\text{Fe}\cdot 0.18\text{B}$ . Experimental data after Russev and Stoyanova [41].

We have also obtained analogous  $a(T)$  dependences with plain Tefzel melts, as well as with a number of oxide and organic polymer glass-forming melts [39]. The values of  $V_m(T)$  (or  $a$ ) estimated from this analysis are always larger than the volume of the expected repeatable structural units. Thus,  $V_m(T)$  is five to ten times larger than  $V_0$  for  $\text{Rb}_2\text{O}/\text{SiO}_2$  (as reported by Li and Uhlmann [26]) and for the  $\text{Na}_2\text{O}/\text{PbO}/\text{Bi}_2\text{O}_3/\text{SiO}_2$  inorganic glasses analysed by us



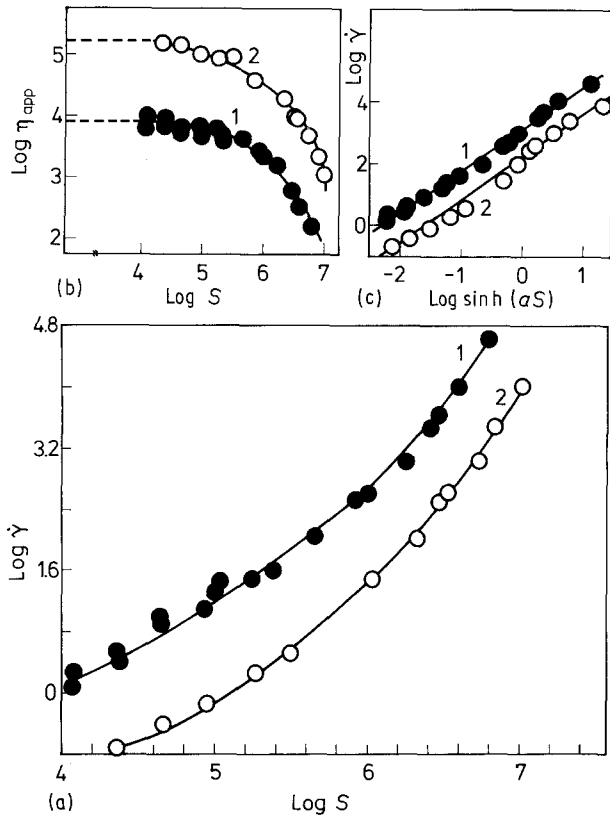


Figure 10 Stress-induced flow of poly(methyl methacrylate) as an example of pseudoplastic non-Newtonian liquid. Experimental data reported by Gul and Kuleznev [42]: (a)  $\log \dot{\gamma}$  versus  $\log S$  data for two temperatures. (b) Determination of the Newtonian viscosity,  $\eta_0$ . (c) The experimental  $\dot{\gamma}(S)$  data in coordinates according to the Prandtl–Eyring model Equation 6a. 1, (●) Data at 523 K; 2, (○) data at 473 K.

[39]. This discrepancy can be explained by introducing flow units consisting of several structural units. However, for the organic polymers mentioned, the respective  $a$  values give  $f^* = 10^2$ – $10^4$ , and it cannot be considered that this is consistent with the idea of a flow unit jumping over a potential barrier in the sense of the Prandtl–Eyring model.

Finally, the flow of water, depicted in Fig. 12, gives a classical example [33, 34] for a dilatant non-Newtonian liquid with  $n = 0.75$ . The observed  $\dot{\gamma}(S)$  dependence is in a qualitative agreement with both Darcy’s empirical formula and Equation 15 (at  $aS < 1$ ).

## 6. Discussion

It appears that the mathematical formalism following from the Prandtl–Eyring model (Equations 6a and b) can be used for a quantitative description of the flow curves for any pseudoplastic liquid. Its use provides a safe determination of  $\eta_0$  even in sufficiently narrow  $S$  intervals where the graphical extrapolation in coordinates  $\log \eta_{\text{app}}$  versus  $\log S$  (see Fig. 10b) cannot be accomplished. Existing empirical formulae for pseudoplastic flow follow from Equations 6a and b and it transpires that this equation describes in a more appropriate way the experimental data than the empirical dependences of the de Waele–Ostwald type, which can be used only in relatively small  $S$  intervals. Practically, all analysed glass-forming melts (with

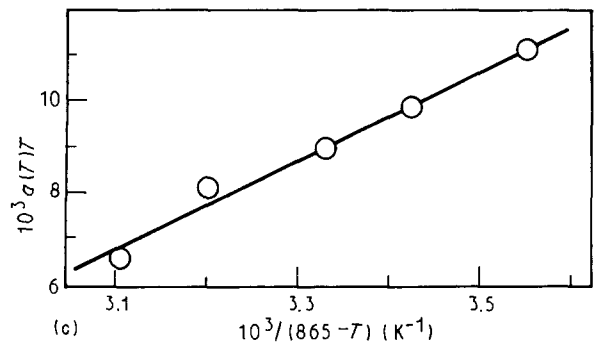
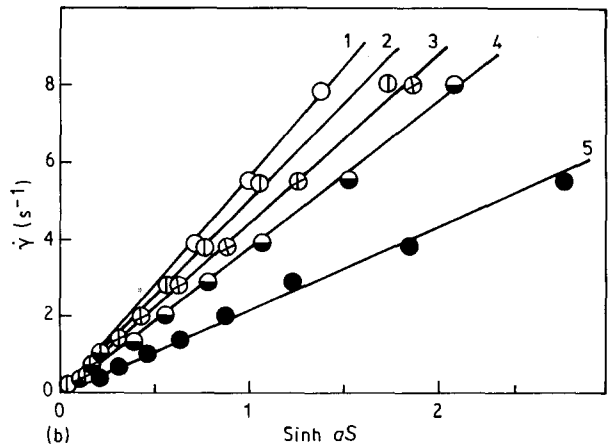
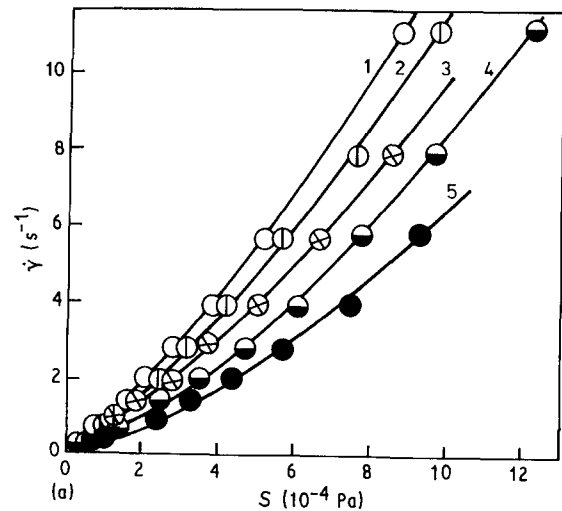


Figure 11 Pseudoplastic non-Newtonian flow of Tefzel melts with 0.3%  $\text{TiO}_2$ . (a)  $\dot{\gamma}(S)$  dependences at five different temperatures according to measurements of Dobreva *et al.* [39]. (b) The same data in terms of the Prandtl–Eyring formula (Equation 6). (c) Temperature dependence of the parameter  $a$  in coordinates  $a(T)T$  versus  $1/(T^* - T)$  in accordance with Equation 19  $T^* \approx 5T_g = 865$  K. 1, 583 K; 2, 573 K; 3, 563 K; 4, 553 K; 5, 543 K.

the exception of water) can be described as pseudoplastic liquids; in terms of the de Waele–Ostwald equation, the obtained  $n$  values are about 1.5 at medium shear stresses.

The classical Prandtl–Eyring model applicable to pseudoplastic flow, accounts only for the enthalpy component of the activated state complex. The extension of this theory to dilatant behaviour, attempted in Section 3, corresponds to the introduction of additional entropy effects (cf. Equation 14). In this sense, the generalization made with Equation 14 and the

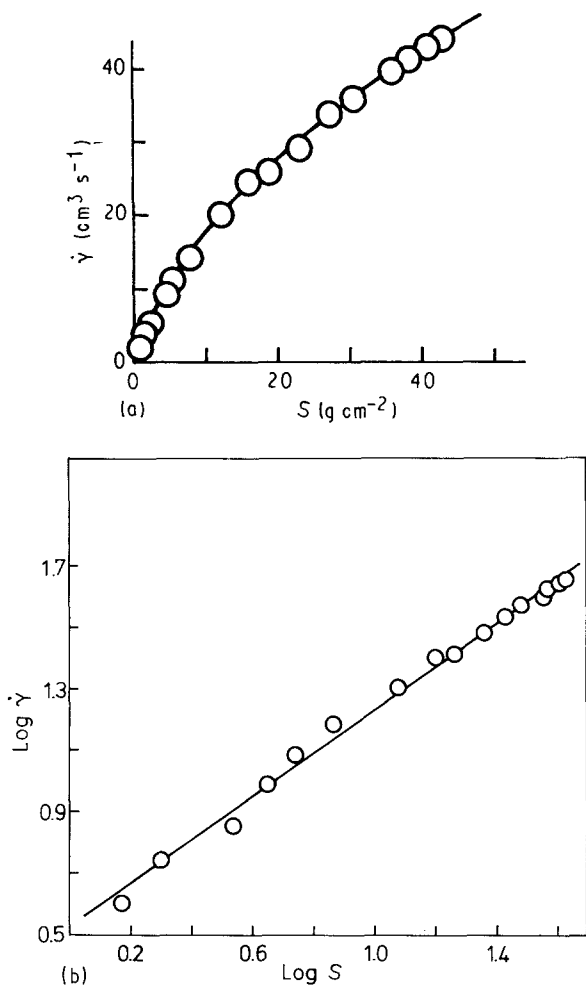


Figure 12 Viscous stress-induced flow of water as an example of a dilatant liquid. (a)  $\dot{\gamma}(S)$  data, after Ostwald [33, 34]. (b) The same experimental evidence in coordinates  $\log \dot{\gamma}$  versus  $\log S$  gives  $n = 0.75$ .

formulae following from it, seems to be a natural and even necessary further development of this classical model.

Dilatant effects are structure dependent. They are of little significance in most polymer melts where the flow of the flexible polymer chains is relatively little inhibited by shear rate. In seemingly simple liquids with asymmetric molecules (cf. the asymmetric aggregative structure of water) dilatant effects may be quite significant.

The superimposition of pseudoplastic and dilatant effects may result in pseudo-Newtonian flow. This pseudolinear dependence can be easily distinguished from the classical Newtonian behaviour: at  $S \rightarrow 0$ , the pseudo-Newtonian dependence does not give  $\dot{\gamma} = 0$  (see Fig. 6).

However, our analysis of the flow curves in terms of the potential barrier model revealed some problems, already indicated by previous investigators [25–27]. Thus the values of the parameter  $a$  are greater than the expected volume of the repeatable structural units,  $V_0$ . In polymer melts, the parameter  $a$  (and thus  $V(T)$ ) reaches such high values (corresponding to  $f^* = 10^2$ – $10^4$ ) that they contradict the very assumptions of the molecular model anticipated with Fig. 2.

However, it can be argued that this result seems to indicate that in polymer melt rheology, the flow of

a whole polymer molecule consisting of thousands of monomeric units, has to be considered. In this connection hydrodynamic coil models have to be recalled, in which the flow kinetics is, in fact, determined by the polymer molecule as a whole [28, 29].

After a simple mathematical rearrangement, Equation 6a can be written in the form (see [19, 20, 25])

$$\frac{\eta_{\text{app}}}{\eta_0} = \frac{\text{arcsinh}(\eta_0 \dot{\gamma} / 2A_0)}{\eta_0 \dot{\gamma}} \quad (21)$$

Expanding the arcsinh function in Equation 21 as

$$\text{arcsinh}(x) \approx x \left( 1 - \frac{1}{6} x^2 \right) \quad (22)$$

and with Equation 2, we arrive at

$$\frac{\eta_{\text{app}}}{\eta_0} \approx 1 - \frac{1}{24} \left[ \frac{V_m(T)}{RT} \dot{\gamma} \right]^2 \quad (23)$$

Equation (23) in its mathematical structure and physical meaning is very similar to the well-known dependence given by Bueche [19, 28] according to which  $\eta_{\text{app}}/\eta_0$  has to be correlated with  $[V_m(T)\dot{\gamma}/RT]^2$ .

The above expansion, and similar considerations, give an indication that probably the Prandtl–Eyring parameter  $a$  has a more general meaning than anticipated by the simple derivation given in the literature [23, 25]. It can be expected that in such terms the enormous  $V_m(T)$  values (or  $f^*$  values) obtained here and by other authors [23, 26, 27] could be explained in a more general formulation of the physical nature of the process of flow in terms of the activated complex theory: as the volume of activated polymer coils, as the volume of dislocations (in the plastic flow of crystals, see [25]) etc.

However, here and in Part II, it is sufficient to state that Equations 6 and 14 give, in fact, the desired formulae applicable to any type of  $\dot{\gamma}(S)$  dependences which will be used further in the analysis of the kinetics of relaxation and retardation.

## Acknowledgement

We thank M.Sc. V. Tonchev for his help in making some of the necessary calculations.

## References

1. G. MOREY, in "Properties of Glass" (Reinhold, New York, 1954) p. 169.
2. M. B. BEAVER, in "Encyclopedia of Material Science and Engineering", Vol. 4, "Mechanical Properties of Polymers" (Pergamon Press, Oxford, 1986) p. 2916.
3. O. V. MAZURIN, in "Vitrification" (Nauka, Leningrad, 1986) in Russian.
4. A. KOVACS, J. AKLONIS, J. HUTCHINSON and A. RAMOS, *Polym. Sci.* **17** (1979) 1097.
5. L. TRELOAR, in "The Physics of Rubber Elasticity" (Clarendon Press, Oxford, 1949).
6. F. KOHLRAUSCH, *Pogg. Ann. Phys. Chem.* **8** (1876) 332.
7. S. M. REKHSOON and O. V. MAZURIN, *J. Amer. Ceram. Soc.* **57** (1974) 327.
8. T. S. CHOW, *J. Mater. Sci.* **25** (1990) 957.
9. G. GOLDBACH and G. REHAGE, *Reol. Acta* **6** (1967) 30.

10. E. JENCKEL, *Z. Electrochem. Angew. Phys. Chem.* **43** (1937) 796.
11. E. JENCKEL, in "Die Physik der Hochpolymeren", edited by A. A. Stuard, 3rd Edn (Springer Verlag, Berlin, 1955) p. 620.
12. E. G. VOSTROKNUTOV and G. V. VINOGRADOV, in "Rheological Foundations of Polymer Processing" (Izd. Chimia, Moscow, 1980) p. 16, in Russian.
13. A. TOBOLSKY, P. POWELL and H. EYRING, in "Chemistry of High Molecules N2", edited by V. A. Kargin (Inostr. Lit., Moscow, 1948) p. 206, in Russian.
14. M. DOI, *J. Polym. Sci. Polym. Phys.* **18** (1980) 1005.
15. *Idem*, *J. Polym. Sci. Polym. Lett.* **19** (1981) 265.
16. I. GUTZOW, A. DOBREVA and J. SCHMELZER, *J. Mater. Sci.* **28** (1993) 901.
17. R. HOUWINK, in "Elastizität, Plastizität und Struktur der Materie" (Verl. Th. Steinkopff, Dresden, 1957) p. 69.
18. T. ALFREY, in "Mechanical Behaviour of High Polymers" (Academic Press, New York, 1948) Ch. 2.
19. S. MIDDLEMANN, in "The Flow of High Polymers" (Academic Press, New York, 1962) Ch. 4.
20. G. VINOGRADOV and A. MALKIN, "Reology of Polymers" (Chimia, Moscow, 1977) p. 150, in Russian.
21. L. PRANDTL, *ZAMM* **8** (1928) 85.
22. A. FREUDENTHAL, in "Inelastisches Verhalten von Werkstoffen" (Techn, Berlin, 1955) pp. 109, 191.
23. S. GLASSTONE, K. LAIDLER and H. EYRING, in "The Theory of Rate Processes" (McGraw-Hill, London, 1941) pp. 480, 513.
24. W. KAUZMANN and H. EYRING, *J. Amer. Chem. Soc.* **66** (1940) 3113.
25. T. REE and H. EYRING, in "Rheology: Theory and Applications", Vol. 2, edited by F. R. Eirich (Academic Press, New York, 1960) p. 83.
26. J. H. LI and D. R. UHLMANN, *J. Non-Cryst. Solids* **3** (1970) 127.
27. M. GOLDSTEIN, *J. Chem. Phys.* **51** (1969) 3728.
28. F. BUECHE, in "Physical Properties of High Polymers" (Interscience, New York, 1962) p. 70.
29. W. GRASSLEY, in "Entanglement Concept in Polymer Rheology", *Advances in Polymer Science*, Vol. 16 (Springer, Berlin, 1974) p. 26.
30. M. DOI and S. F. EDWARDS, *J. Chem. Soc. Farad. Trans. 2* **74** (1978) 1789.
31. E. JANKE, F. EMDE and L. LOSCH, in "Tafeln hoherer Funktionen" 6 Edn. (Teubner, Stuttgart, 1960).
32. R. V. TORNER, in "Theory of Polymer Processing" (Chimia, Moscow, 1972) p. 47, in Russian.
33. W. OSTWALD, *Kolloid Z.* **47** (1929) 176.
34. *Idem*, *ibid.* **36** (1925) 99.
35. W. L. WILLKINSON, in "Non Newtonian Fluids, Fluid Mechanics, Mixing and Heat Transfer" (Pergamon Press, London, 1960) Ch. 1.
36. G. M. BARTENEV, *Vysoko Moleculiarnie Soedinenia* **6** (1964) 2155.
37. D. M. HEYES, J. J. KIM, C. J. MONTRO and T. A. LITOVITZ, *J. Chem. Phys.* **73** (1980) 3987.
38. J. R. PARTINGTON, in "An Advanced Treatise on Physical Chemistry", Vol. 2 (Longmans Green, London, 1955) p. 43.
39. A. DOBREVA, D. GEORGIEV, A. NIKOLOV and I. GUTZOW, paper submitted for publication.
40. R. WÄSCHE and R. BRÜCKNER, *ibid.* **27** (1986) 80.
41. K. RUSSEW and I. STOYANOVA, *J. Mater. Sci. Engng* **A123** (1990) 80.
42. N. E. GUL and V. N. KULEZNEV, in "Structure and Mechanical Properties of Polymers" (Vish. Shkola, Moscow, 1966) p. 171, in Russian.

*Received 18 December 1991  
and accepted 25 June 1992*